View metadata, citation and similar papers at core.ac.uk

brought to you by CORE

provided by NASA Technical Reports Server

NASA/TM—1998-207420

AIAA–98–3252

Transmission and Incidence Losses for a Slotted Plate

Jack Wilson
NYMA Inc., Brook Park, Ohio

Rodrick V. Chima
Lewis Research Center, Cleveland, Ohio

Beric W. Skews
University of the Witwatersrand, Johannesburg, South Africa

Prepared for the
34th Joint Propulsion Conference and Exhibit
cosponsored by AIAA, ASME, SAE, and ASEE
Cleveland, Ohio, July 13–15, 1998

National Aeronautics and
Space Administration

Lewis Research Center

June 1998

Available from

NASA Center for Aerospace Information
7121 Standard Drive
Hanover, MD 21076
Price Code: A03

National Technical Information Service
5287 Port Royal Road
Springfield, VA 22100
Price Code: A03

TRANSMISSION AND INCIDENCE LOSSES FOR A SLOTTED PLATE

Jack Wilson*
NYMA, Inc.
Brook Park, Ohio 44142

Rodrick V. Chima†
National Aeronautics and Space Administration
Lewis Research Center
Cleveland, Ohio 44135

and

Beric W. Skews
University of the Witwatersrand
Johannesburg, South Africa

Abstract

The objective of this work is to find a model of the stagnation pressure loss resulting from flow through a slotted plate, which is effectively a cascade of flat plate airfoils, particularly at very large angles of incidence. Data from a published experiment is examined, and compared with control volume analysis, and CFD code calculations. An assumption that the loss can be separated into a transmission loss and an incidence loss seems to be justified by the data. Both the data and the CFD code results are consistent with an incidence loss model in which the flow component normal to the slot axis is lost. However, the experimental transmission loss is much larger than calculated values.

Nomenclature

b	distance between centerlines of neighboring slots
F	momentum of flow
H	stagnation enthalpy
K	pressure loss coefficient = $\Delta P/0.5\ \rho\ V^2$
ℓ	plate thickness
M	Mach number of flow incident on the slot
M_s	Mach number of shock wave generating the flow
m	mass flow rate
P	stagnation pressure of flow
p	static pressure of flow
ΔP	change in stagnation pressure across the slot
V	velocity of flow incident on the slot
t	web thickness
α	angle of incidence of flow relative to slot axis
β	blockage, i.e., t/b
β^*	effective blockage at vena contracta
γ	ratio of specific heats
ρ	density of air
φ	contraction coefficient = $(1 - \beta^*)/(1 - \beta)$

Subscripts

1	value upstream of the slot
2	value at vena contracta
3	value at passage exit
4	value downstream of slot (mixed out)

*Senior Member, AIAA
†Associate Fellow, AIAA

Introduction

The rotor used in a wave rotor has axial passages arranged around the circumference of a drum. Air enters the passages via ducts, which span several passages. The leading edge of a duct is frequently rounded to minimize losses due to vortex shedding, but this can result in the air being incident on the rotor at large angles of attack,[1] which may approach 90°. Flow at high angles of attack will suffer a loss of stagnation pressure, called incidence loss. Air entering the passages without incidence will also undergo a stagnation pressure loss due to the drag of the walls on the flow. This loss is termed transmission loss here. Accurate modelling of wave rotor performance requires knowledge of both these losses. Unfortunately, there does not appear to be much data in the literature on incidence losses at high angles of attack.

The flow into the wave rotor may be idealized as the flow into a cascade of flat plate airfoils at zero stagger angle. This geometry is shown in Fig. 1. Passages of length ℓ, and height (b-t) are formed by webs, of thickness t, whose centerlines are spaced a distance b apart. There is an incident flow of Mach number M, at an angle of incidence α. The thickness of the webs is greatly exaggerated in Fig. 1 in comparison with a wave rotor, where the value of t/b would be of the order of 10 percent or less. Also the passages would be much longer in a wave rotor than those shown. In most aerodynamic flows, the angles of incidence are kept small deliberately, accounting for the paucity of data at high values of incidence. Emmert has given data for turbine blades, with turbine style airfoils rather than flat plates,[2] up to incidence angles of 60°. The origin of these data was not quoted, so it is difficult to assess their validity. Two limiting curves were given, for sharp-nosed and round-nosed airfoils, without defining either term. Any given airfoil could presumably lie anywhere between these two curves. These curves are reproduced in Fig. 2. More recently, Moustapha et al.[3] have attempted to correlate data from many turbine cascade experiments, taking the blade geometry into account. Using a geometry from their in-house experiments, a curve of loss coefficient versus angle of incidence can be generated from the correlation given by Moustapha et al., and is also shown in Fig. 2. The maximum angle in their tests was 30°. There are two additional curves shown in Fig. 2. One, labelled $K = \sin^2(\alpha)$, corresponds to the value obtained by assuming that the component of velocity normal to the slot is completely lost,[4] an assumption that is frequently made.The other curve, labelled $K = \sin^3(\alpha)$, has no theoretical validity, but does appear to be a good fit to Emmert's data at angles of incidence above 30°. It is clear from these data that there is no agreement on the dependance of the loss coefficient on angle of incidence.

For the geometry of interest, there are data for incompressible flow, listed by Idelchik.[5] These data were taken with flows of water in open channels, and are not applicable to confined compressible flows. There are also data for screens by Cornell,[6] which do encompass the desired Mach number range, but the data are only for normal incidence, for screens of wire mesh, rather than finite length passages. Cornell did find that the loss was quite strongly dependant on Mach number, particularly at high values of solidity, but only very weakly on Reynolds number, for Reynolds numbers in the range 10^2 to 10^5, based on wire diameter. In a recent, experiment, Skews and Takayama[7] have studied the reflection of shock waves by porous surfaces, passing shock waves over a slotted plate in a shock tube. The measured data permitted calculation of the loss in stagnation pressure for flow through the plate. In their work, incidence values varied from 0° to 75°. The object of the present paper is to examine these data, evaluate the pressure loss, and determine the relative contributions of incidence loss and transmission loss. It did not prove possible to determine the dependance of incidence loss on angle of incidence.

Loss Measurements

The experiments of Skews and Takayama[7] consisted of a set of measurements in a shock tube in which a shock wave was passed over a slotted plate, set at various angles to the shock tube axis. A sketch of the plate is given in Fig. 3. Actually, two plates were used, with different values of blockage. One, with a blockage of 0.6, was called the coarse plate; the other, with a blockage of 0.67, was called the fine plate. Figure 1 is a scale drawing of the passages of the coarse plate. Although the experiment itself was unsteady, the flow through the plate was steady, in the plate reference frame, for the duration of the test time. The shock speed, M_s, was very well controlled, and three different values were used, giving inverse pressure ratios of 0.4, 0.5, and 0.7. Values of the velocity and angle of the flow incident on the plate were derived from photographs of the flow. These photographs were made by double exposure holographic interferometry; examples are given in Fig. 4. Similarly, from measurements of the angle of the shock wave emerging from the back-side of the plate, it proved possible to calculate the pressure, velocity, and Mach number of this flow. Hence the static pressure loss across the plate was found. The details are in Skews and Takayama.[7] By evaluating the Mach number on each side of the plate, the static pressure loss can be converted to stagnation pressure loss. The incident Mach number, angle of incidence, and stagnation pressure loss divided by incident stagnation pressure are given in Table I. The stagnation pressure drop as found for each value of incident shock speed, is plotted in Fig. 5 against incidence angle.

The number printed beside some of the data points is the Mach number of the flow incident on the slot in the slot frame of reference. It will be seen that the pressure drop at zero incidence (i.e., flow normal to the plate) is much larger than the change in pressure drop due to incidence. However, the change in stagnation pressure drop with incidence is complicated by the fact that the flow Mach number is increasing as well as the angle of incidence. The flow Reynolds Numbers, based on web thickness, were around 2.6×10^3 to 5×10^3, so should have been in the range for which the loss is independant of Reynolds Number.

Transmission Loss at Zero Incidence

The loss of stagnation pressure across the plate will be assumed to have two components, a transmission loss, and an incidence loss. The transmission loss is caused by the flow being necked down in the slot, undoubtedly with a vena contracta, and then expanded as it leaves the slot. The incidence loss is the loss caused by the fact that the flow is approaching the slot at an angle of incidence. It will be assumed that these two losses are additive, though it is by no means obvious that this is so.

Experimental Transmission Loss

Clearly, the observed loss is the transmission loss when the angle of incidence is zero. Thus the cases from Table I for which the angle of incidence is zero are plotted in Fig. 6 as transmission loss versus incident Mach number. In addition, cases for $\beta = 0.6$ for which the angle of incidence was less than 35° are also plotted in Fig. 6, as open squares. It will be shown later that incidence loss is negligible for these cases, so the loss measured for these cases is also transmission loss. Fitting a power law to these points by the method of least squares results in the expression;

$$\Delta P/P_1 = 1.27\,M^{0.563} \tag{1}$$

for the coarse grid, and

$$\Delta P/P_1 = 1.96\,M^{0.666} \tag{2}$$

for the fine grid. These formulae are plotted as the dashed lines in figure 6.

Calculated Transmission Loss

Control Volume Analysis. An estimate of the transmission loss can be made by solving the mass, momentum, and energy equations for one-dimensional flow. The flow is broken into three sections: (1) from far upstream to the vena contracta, (2) from the vena contracta to the passage exit, and (3) from the exit to far downstream. In region 1, it is assumed that the front wall of the web will be entirely at the stagnation pressure of the flow, so that it provides a drag on the flow. In addition, the flow will neck down to a vena contracta, and the area between the web and the vena contracta will also be assumed to be at the upstream stagnation pressure, providing further drag. This is undoubtedly an overestimate of the drag force, but is done to obtain the maximum loss. The momentum equation becomes, taking the upstream area to be unity;

$$F = mV_1 + p_1 - P_1\beta^* = mV_2 + p_2(1-\beta^*) \tag{3}$$

This can be combined with the perfect gas law, mass conservation, and energy conservation, following Foa[8], to give a quadratic equation which can be solved for z, where

$$z_2 = \sqrt{1-2\left(\left(\gamma^2-1\right)/\gamma^2\right)\left(m^2H/F^2\right)} \tag{4}$$

$$= \sqrt{1-\frac{2(\gamma+1)M_1^2\left(1+\left((\gamma-1)/2\right)M_1^2\right)}{\left(1+\gamma M_1^2-\left(P_1/p_1\right)\beta^*\right)^2}} \tag{5}$$

and the Mach number follows from;

$$M_2 = \sqrt{(1-z_2)/(1+\gamma z_2)} \tag{6}$$

With the Mach number determined, the static pressure is found from the continuity equation, and hence the stagnation pressure. What is unknown up to this point is the value of β^*, or equivalently, the contraction coefficient φ. Values of φ were derived from the plots given by Cornell,[6] by interpolating for $\beta = 0.6$ and 0.67, and fitting these with parametric equations in β and pressure ratio. The approximate value of φ was 0.75.

Similarly, at the exit of the passages, it is assumed that the flow has filled the passage uniformly, and then expands downstream to fill the total open area.

The momentum equation becomes:

$$F = mV_3 + p_3 = mV_4 + p_4 \tag{7}$$

and the solution is;

$$z_4 = \sqrt{1-\frac{2(\gamma+1)M_3^2(1-\beta)^2\left(1+\left((\gamma-1)/2\right)M_3^2\right)}{\left(1+\gamma M_3^2(1-\beta)\right)^2}} \tag{8}$$

A similar solution exists between the vena contracta and the passage exit. Putting all three regions together gives the drop in stagnation pressure through the passage. This has been plotted as a function of upstream Mach number in Fig. 6, for comparison with the data. The agreement with the data is poor, with the observed loss significantly greater than the calculated loss. The calculated loss can be made to agree with the data by using very low values of the contraction coefficient, from $\varphi = 0.31$ at $M_1 = 0.05$, to $\varphi = 0.63$ at $M_1 = 0.12$, but these values seem extremely low.

CFD. The RVCQ3D Navier Stokes CFD program of Chima,[8] was used to calculate the flow in the slots for $\beta = 0.6$, for a variety of Mach numbers, for flow normal to the plate (i.e., $\alpha = 0$). The flow was entirely subsonic for incident Mach numbers less than 0.2. For flows above this value, the flow becomes sonic at the vena contracta, then accelerates to supersonic flow at the passage exit, and beyond. The subsonic flows presented a mathematical difficulty downstream of the slot. The actual flow undoubtedly contains shed vortices, and so is inherently unsteady. As a result, it was not possible to obtain a solution downstream of the slot, although it was possible to find a solution at the exit plane. The exit static pressure and distribution of Mach number were then used as input to a control volume calculation to determine the stagnation pressure far downstream of the slot. The resulting pressure loss is plotted in Fig. 6. It can be seen that this calculated loss is even lower than the loss calculated with the control volume analysis, and much lower than the observed values. The loss does rise rapidly once the flow becomes supersonic. However, all the observed pressure drops are for incident Mach numbers for which the CFD calculation indicates that the flow should be subsonic.

Incidence Loss

As stated in the introduction, it is sometimes assumed (Ref. 4) in turbine work that flow impacting an airfoil at incidence will suffer a loss of kinetic energy equal to the component of kinetic energy normal to the chord, i.e.;

$$\text{Kinetic Energy Loss} = [V\sin(\alpha)]^2/2 \qquad (9)$$

Although this is not necessarily the correct dependance on incidence angle, it will be used here for simplicity. The loss of stagnation pressure follows as;

$$\Delta P|_{inc} = 0.5\rho V^2 \sin^2(\alpha) \qquad (10)$$

from which;

$$\left.\frac{\Delta P}{P_1}\right|_{inc} = \frac{\gamma M_1^2 \sin^2(\alpha)}{2\left[1+\left(\frac{\gamma+1}{2}\right)M_1^2\right]^{\gamma/(\gamma-1)}} \qquad (11)$$

This formula has been used to calculate an incidence loss for each of the experimental points; the results are in Table I. It will be seen that , as stated above, the incidence loss for angles of incidence less than 35° is very small compared with the measured total loss.

The CFD code was used to calculate flows approaching a slot of $\beta = 0.6$ at angles of incidence of 0°, 30°, 45°, 60°, and 75°, for incident Mach numbers which gave an axial Mach number component (i.e., $M\cos(\alpha)$) of approximately 0.2. Mach number contours of these flows, for $\alpha = 0, 30°$, and 75°, are given in Fig. 7. It will be seen that the flow is extremely complex. The flow separates on going round the sharp inlet corner, giving rise to separation bubbles, which reattach downstream. As a consequence, there is a throat between the bubbles, and the flow chokes close to the inlet, and then accelerates to slightly supersonic speeds downstream of the bubbles. As the incidence is increased, the separation bubble on the suction side increases, but that on the pressure side decreases. The losses grow as the incidence increases, and the minimum axial Mach number which causes choking decreases. Above about $\alpha = 60°$, shocks form within the slot causing an increase in losses. The exit flow expands to a low pressure, and is surprisingly insensitive to incidence. All cases had supersonic flow downstream, and it was possible to calculate a total stagnation pressure loss from the solution. These values of stagnation pressure loss are given in Fig. 8. Also given in Fig. 8 are points generated by assuming that all points had a transmission loss equal to that calculated with the code for normal flow at an incident Mach number of 0.2, and an incidence loss given by Eq. (11). There is quite good agreement between the two curves. In fact, for the cases chosen, the axial component of Mach number decreased somewhat as the angle of incidence increased. Thus the transmission loss should decrease as the angle of incidence increases. If this could be properly accounted for, the agreement would be even better. These results indicate that the CFD code is not inconsistent with the assumptions above, namely that;

(1) the incidence loss is described by Eq. (11)
(2) the transmission and incidence losses are additive.

Total Loss

The total loss for the case of a plate with a flow at an angle of incidence will be assumed to be the sum of the incidence loss as calculated above, and a transmission loss

calculated with formula (1) for the coarse grid, or formula (2) for the fine grid , but using the component of the flow Mach number normal to the plate, i.e., Mcos(α) rather than the Mach number itself. For the coarse grid the total loss will then be:

$$\frac{\Delta P}{P_1} = 1.27\left(M_1 \cos(\alpha)\right)^{0.563} + \frac{\gamma M_1^2 \sin^2(\alpha)}{2\left[1+\left(\frac{\gamma-1}{2}\right)M_1^2\right]^{\gamma/(\gamma-1)}} \tag{12}$$

If this is a valid model of the total loss, then a plot of transmission loss against Mcos(α) should fall on a single line. In Fig. 9, the experimental total loss, minus the calculated incidence loss, is plotted against $M_1 \cos(\alpha)$, for both the coarse grid and the fine grid. Whilst there is considerable scatter in the data, the data do collapse to a single line. Alternatively, the measured total loss can be plotted against the incident Mach number, and compared with curves of total loss calculated from the sum of transmission loss and incidence loss, using Eq. (12). Such a plot is shown in Fig. 10, for the coarse grid. There is not perfect agreement between data and experiment, nor could there be, given the spread of the experimental data, but the trends do appear to be correct.

Discussion

What is rather surprising about the results is the significant reduction in total pressure loss at a given incident Mach number with increasing angle of incidence. For the particular slotted plates used, the transmission loss dominated over the incidence loss, so this result seems to be a consequence of the reduction in the component of Mach number normal to the plate as the incidence is increased. Use of the normal component of Mach number to characterize the loss seems reasonably accurate. The incidence loss is too small to reach any conclusions about its dependance on angle or Mach number other than to say that it is not inconsistent with Eq. (11). This is true both from the experimental results, and the CFD calculations. The major discrepancy between calculation and experiment seems to be the large value of transmission loss observed for flow normal to the plates at quite low incident Mach numbers, such that the flow is entirely subsonic. This discrepancy could be explained if the contraction coefficient were actually much lower than the values assumed in the control volume analysis, or implicitly calculated in the CFD calculations. It is worth noting that measurements of the loss coefficient of cascades of turbine blades as a function of Mach number made by Schlichting and Das, as reported in Schlichting,[10] show a dependance on Mach number similar to that of the present calculations for high Reynolds' number, for which the flow remains attached. At low Reynolds' number, the flow separates, and the dependance of the loss coefficient on Mach number becomes almost linear with Mach number, similar to the results of Skews and Takayama, as shown in Fig. 6. The flow is undoubtedly very complex, and it is probably wishful thinking to expect it to be modelled simply.

As stated above, the plates used to generate the experimental results exhibited more transmission loss than incidence loss, having open air ratios of only 33 and 40 percent. However, the technique is by no means limited to such plates, and, by using a more open plate, it is possible that data could be generated in which the incidence loss dominates, so that such losses could be characterized by Mach number and incidence angle.

References

1. Welch, G.E., "Computational Model for Wave Rotor Flow Dynamics," *Journal of Engineering for Gas Turbines and Power*, Vol. 119, pp. 978–985, October 1997.
2. Emmert, H.D., "Current Design Practices for Gas-turbine Power Elements," *Trans ASME*, Vol. 72, No. 2, pp. 189–200, February 1950.
3. Moustapha, S.H., Kacker, S.C., and Tremblay, B., "An Improved Incidence Losses Prediction Method for Turbine Airfoils," *Journal of Turbomachinery*, Vol. 112, pp. 267–276, April, 1990.
4. Roelke, R.J., "Miscellaneous Losses," Chapter 8 of *Turbine Design and Application*, NASA SP–290, Vol. 2, pp. 125–148, 1994.
5. Idelchik, I.E., *Handbook of Hydraulic Resistance.* Hemisphere Publishing Corporation, New York, N.Y. 1986.
6. Cornell, W.G., "Losses in flow normal to plane screens," *Trans. ASME*, No. 4, pp. 145–153, 1958.
7. Skews, B.W. and Takayama, K., "Flow through a perforated surface due to shock wave impact," *J. Fluid Mech.*, Vol. 314, pp. 27–52, 1996.
8. Foa, J.V., *Elements of Flight Propulsion*, John Wiley & Sons, Inc. New York, N.Y. 1960.
9. Chima, R.V., "Explicit Multigrid Algorithm for Quasi-Three-Dimensional Viscous Flows in Turbo-machinery," *J. Propulsion and Power*, Vol. 3, No. 5, pp. 397–405, Sept-Oct , 1987.
10. Schlichting, H., *Boundary-Layer Theory*, McGraw-Hill Book Company, New York, N.Y. 1979, p. 774.

TABLE I(a).—DATA FROM THE EXPERIMENT BY SKEWS AND TAKAYAMA[7] FOR THE COARSE GRID

α	M_1	Observed stagnation pressure drop	Pressure drop due to incidence	Transmission stagnation pressure drop
0	0.069	0.261	0	0.261
0	.123	.383	0	.383
0	.152	.404	0	.404
26.3	0.167	0.446	0.004	0.442
26.6	.080	.288	.001	.287
31.3	.120	.420	.003	.417
33.2	.070	.259	.001	.258
47.3	0.192	0.473	0.014	0.459
48.3	.101	.327	.004	.323
48.5	.159	.488	.010	.478
53.1	.269	.479	.031	.448
55.6	.131	.313	.008	.305
60.0	0.210	0.482	0.022	0.460
61.8	.325	.522	.053	.469
63.9	.487	.496	.114	.382
64.6	.264	.467	.038	.429
67.0	0.158	0.292	0.015	0.277
68.6	.445	.519	.162	.414
70.0	.250	.313	.037	.276
70.6	.250	.337	.037	.300
71.0	.336	.477	.065	.412
71.4	.275	.292	.045	.247
71.7	.509	.551	.137	.414
71.8	.315	.483	.059	.424
72.4	.223	.313	.031	.282
73.3	.575	.557	.170	.387
73.9	.305	.285	.056	.229
75.4	.423	0.508	0.104	0.404
76.4	.481	.508	.113	.377

TABLE I(b).—DATA FROM THE EXPERIMENT BY SKEWS AND TAKAYAMA FOR THE FINE GRID

α	M_1	Observed stagnation pressure drop	Pressure drop due to incidence	Transmission stagnation pressure drop
0	0.067	0.308	0	0.308
0	.124	.471	0	.471
47.0	0.105	0.353	0.004	0.349
57.0	.176	.509	.015	.494
64.3	.162	.336	.015	.321
67.0	0.312	0.545	0.054	0.491
72.6	.221	.348	.030	.318
73.8	.449	.565	.113	.452

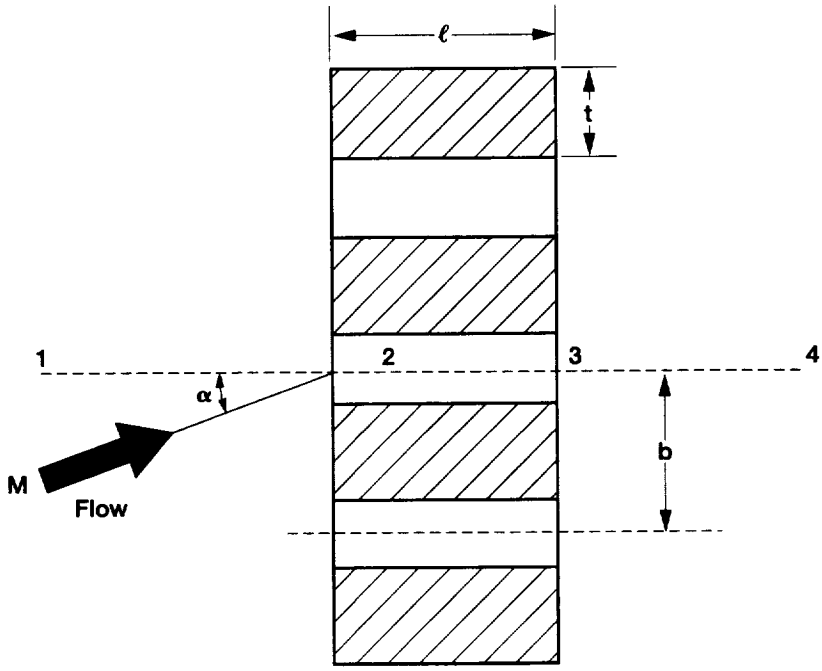

Figure 1.—Flow geometry.

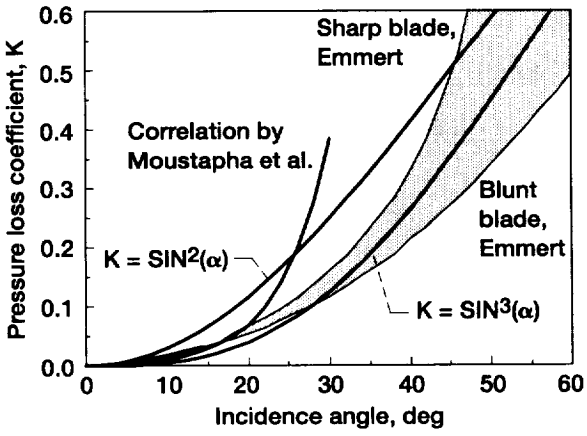

Figure 2.—Stagnation pressure loss coefficient as a function of angle of incidence for turbines and cascades of turbine airfoils.

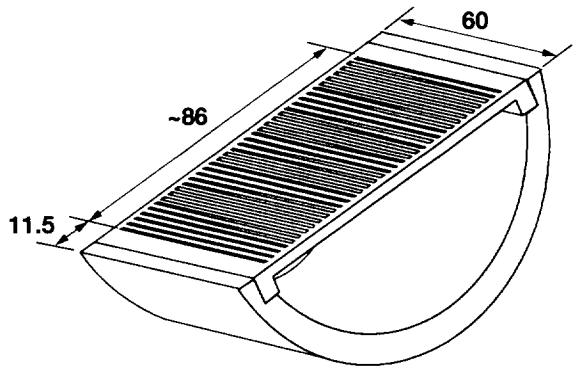

Figure 3.—Model used in the experiments of Skews and Takayama. Dimensions are in mm. This figure is reproduced from reference 7 by kind permission of the Journal of Fluid Mechanics.

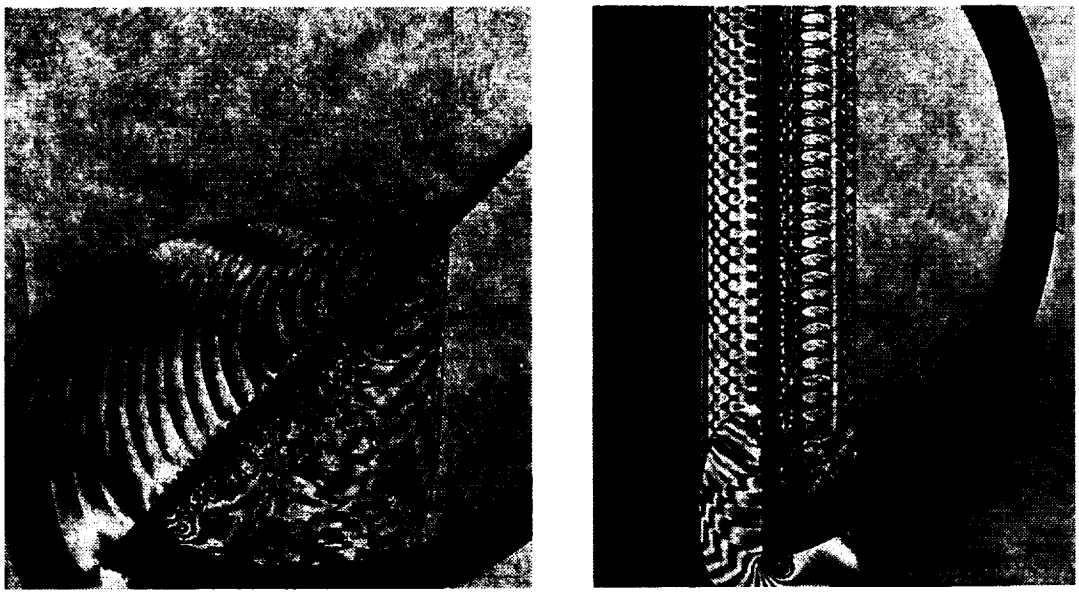

Figure 4.—Interferograms of the flow through the plate taken by Skews and Takayama, showing inclined flow (left), and normal flow (right). These photographs are reproduced from reference 7 by kind permission of the Journal of Fluid Mechanics.

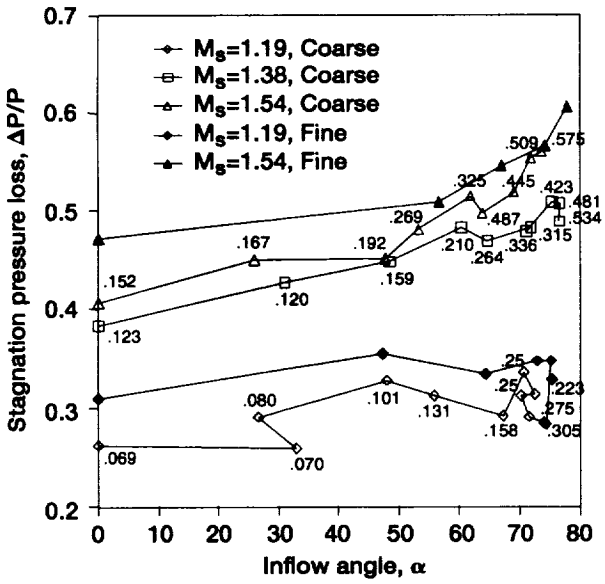

Figure 5.—Values of stagnation pressure drop observed by Skews and Takayama plotted against angle of incidence. The number next to various points indicates the incident Mach number for that point.

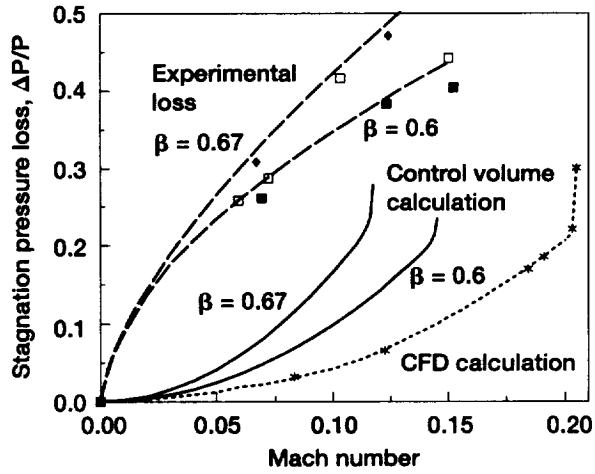

Figure 6.—Transmission stagnation pressure loss for the coarse and fine plates. All points are for $\alpha = 0$, except for the open squares, which are for small values of α, i.e. less than 35°, at $\beta = 0.6$.

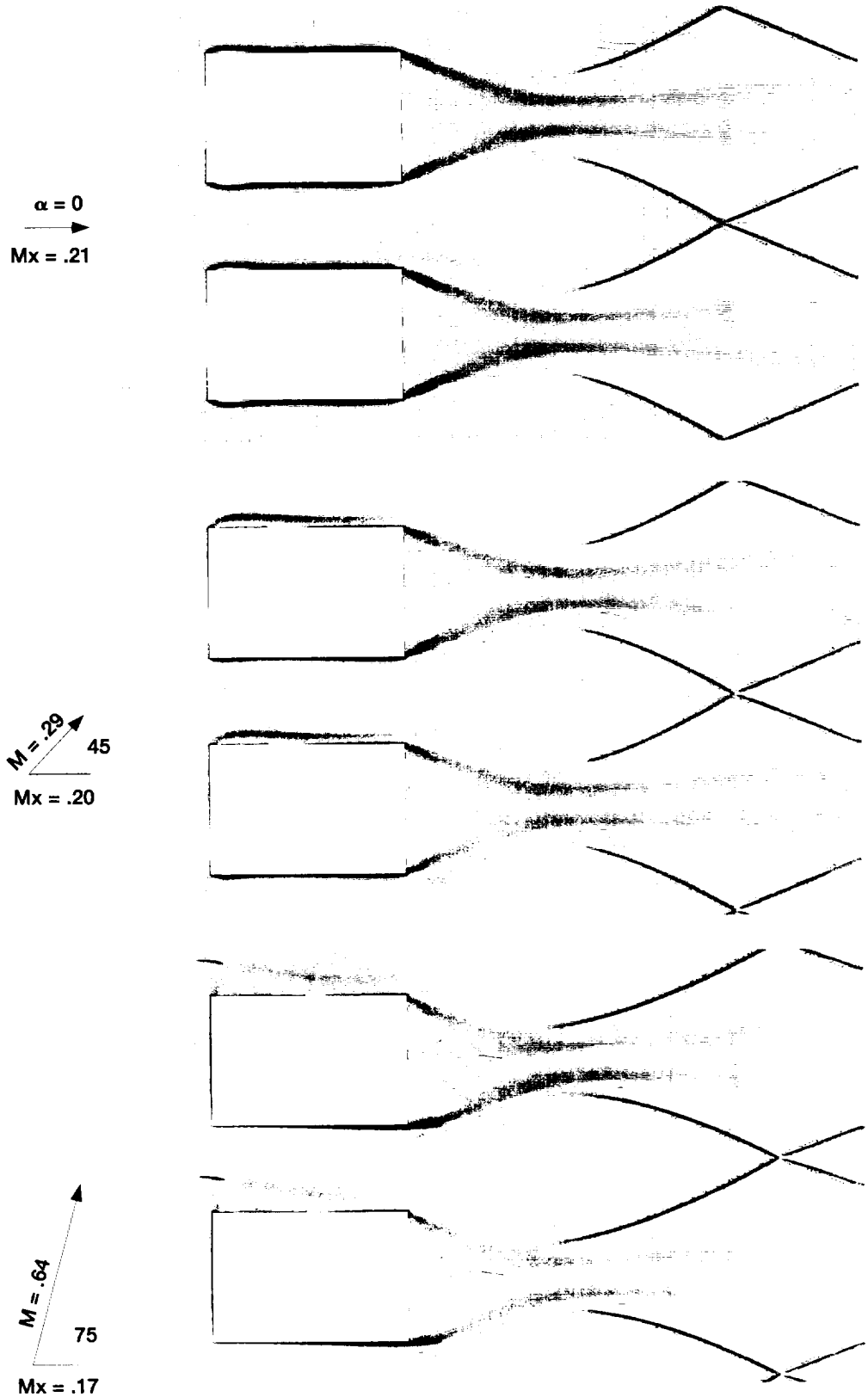

Figure 7.—Mach number contours for the flow through the coarse grid as calculated using CFD, for angles of incidence of 0°, 45°, and 75°.

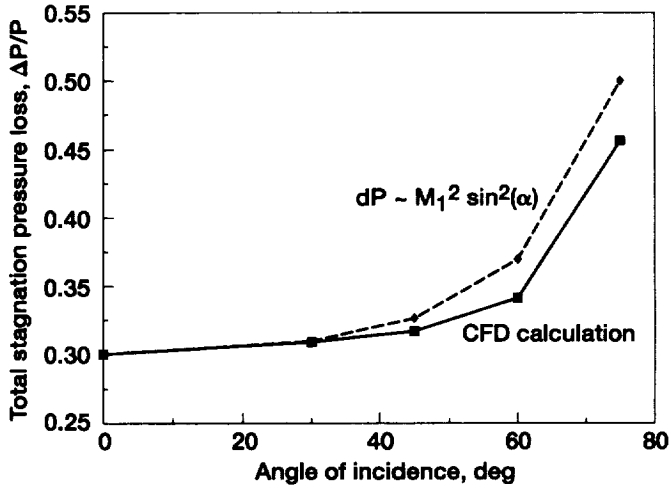

Figure 8.—Comparison of the incidence loss as calculated with equation (11), and as found from CFD calculations.

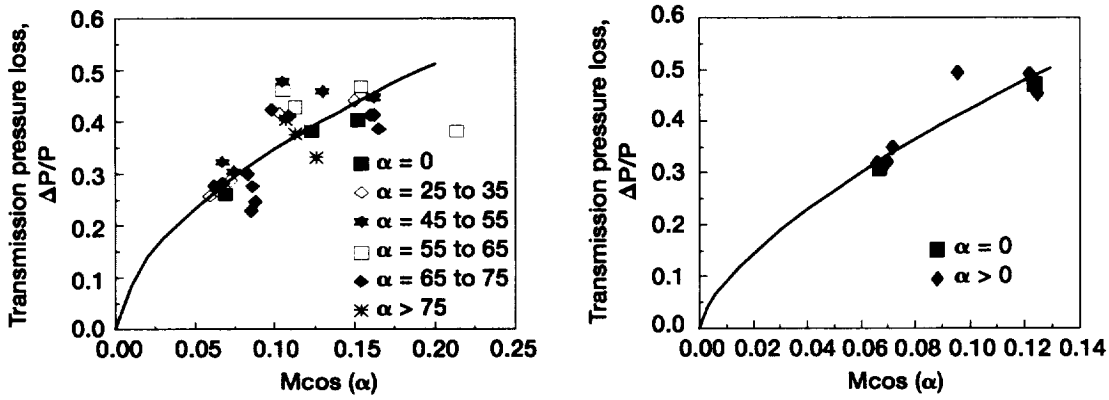

Figure 9.—Transmission pressure drop for the coarse grid (left) and the fine grid (right) plotted against Mcos(α).

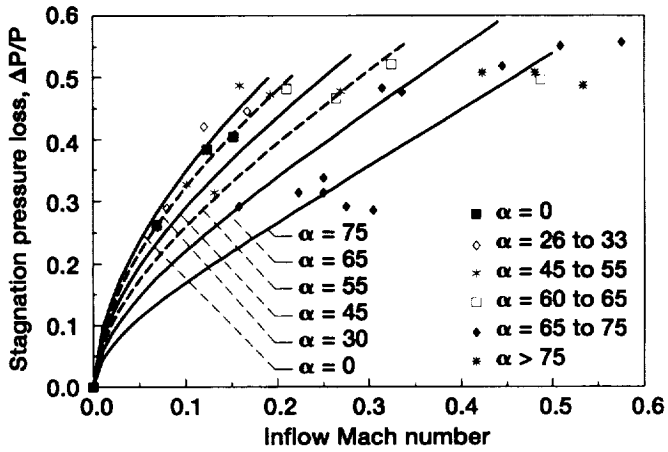

Figure 10.—Experimental and calculated total stagnation pressure drop for the coarse grid plotted against the flow Mach number.

REPORT DOCUMENTATION PAGE

Form Approved
OMB No. 0704-0188

Public reporting burden for this collection of information is estimated to average 1 hour per response, including the time for reviewing instructions, searching existing data sources, gathering and maintaining the data needed, and completing and reviewing the collection of information. Send comments regarding this burden estimate or any other aspect of this collection of information, including suggestions for reducing this burden, to Washington Headquarters Services, Directorate for Information Operations and Reports, 1215 Jefferson Davis Highway, Suite 1204, Arlington, VA 22202-4302, and to the Office of Management and Budget, Paperwork Reduction Project (0704-0188), Washington, DC 20503.

1. AGENCY USE ONLY (*Leave blank*)	2. REPORT DATE	3. REPORT TYPE AND DATES COVERED
	June 1998	Technical Memorandum

4. TITLE AND SUBTITLE

Transmission and Incidence Losses for a Slotted Plate

5. FUNDING NUMBERS

WU–523–26–13–00

6. AUTHOR(S)

Jack Wilson, Rodrick V. Chima and Beric W. Skews

7. PERFORMING ORGANIZATION NAME(S) AND ADDRESS(ES)

National Aeronautics and Space Administration
Lewis Research Center
Cleveland, Ohio 44135–3191

8. PERFORMING ORGANIZATION REPORT NUMBER

E–11175

9. SPONSORING/MONITORING AGENCY NAME(S) AND ADDRESS(ES)

National Aeronautics and Space Administration
Washington, DC 20546–0001

10. SPONSORING/MONITORING AGENCY REPORT NUMBER

NASA TM—1998-207420
AIAA–98–3252

11. SUPPLEMENTARY NOTES

Prepared for the 34th Joint Propulsion Conference and Exhibit cosponsored by AIAA, ASME, SAE, and ASEE, Cleveland, Ohio, July 13–15, 1998. Jack Wilson, NYMA Inc., 2001 Aerospace Parkway, Brook Park, Ohio 44142 (work funded by NASA Contract NAS3–27186). Rodrick V. Chima, NASA Lewis Center, and Beric W. Skews, University of the Witwatersrand, Johannesburg, South Africa. Responsible person, Rodrick V. Chima, organization code 5810, (216) 433–5919.

12a. DISTRIBUTION/AVAILABILITY STATEMENT

Unclassified - Unlimited
Subject Category: 02 Distribution: Nonstandard

This publication is available from the NASA Center for AeroSpace Information, (301) 621–0390.

12b. DISTRIBUTION CODE

13. ABSTRACT (***Maximum 200 words***)

The objective of this work is to find a model of the stagnation pressure loss resulting from flow through a slotted plate, which is effectively a cascade of flat plate airfoils, particularly at very large angles of incidence. Data from a published experiment is examined, and compared with control volume analysis, and CFD code calculations. An assumption that the loss can be separated into a transmission loss and an incidence loss seems to be justified by the data. Both the data and the CFD code results are consistent with an incidence loss model in which the flow component normal to the slot axis is lost. However, the experimental transmission loss is much larger than calculated values.

14. SUBJECT TERMS

Incidence loss; Pressure drop; Cascade

15. NUMBER OF PAGES

16

16. PRICE CODE

A03

17. SECURITY CLASSIFICATION OF REPORT	18. SECURITY CLASSIFICATION OF THIS PAGE	19. SECURITY CLASSIFICATION OF ABSTRACT	20. LIMITATION OF ABSTRACT
Unclassified	Unclassified	Unclassified	